

# Steady-State and Laser Flash Photolysis Study of the Carbon–Carbon Bond Fragmentation Reactions of 2-Arylsulfanyl Alcohol Radical Cations

Enrico Baciocchi,<sup>\*,†</sup> Tiziana Del Giacco,<sup>\*,‡</sup> Fausto Elisei,<sup>‡</sup> Maria Francesca Gerini,<sup>†</sup> Andrea Lapi,<sup>†</sup> Prisca Liberali,<sup>†</sup> and Barbara Uzzoli<sup>‡</sup>

*Dipartimento di Chimica, Università “La Sapienza”, P.le A. Moro 5, 00185 Rome, Italy, and Dipartimento di Chimica and Centro di Eccellenza Materiali Innovativi Nanostrutturati (CEMIN), Università di Perugia, V. Elce di Sotto 8, 06123, Perugia, Italy*

enrico.baciocchi@uniroma1.it; dgiacco@unipg.it

Received August 4, 2004

The *N*-methylquinolinium tetrafluoroborate (NMQ<sup>+</sup>)-sensitized photolysis of the *erythro*-1,2-diphenyl-2-arylsulfanylethanol **1–3** (**1**, aryl = phenyl; **2**, aryl = 4-methylphenyl; **3**, aryl = 3-chlorophenyl) has been investigated in MeCN, under laser flash and steady-state photolysis. Under laser irradiation, the formation of sulfide radical cations of **1–3**, in the monomeric ( $\lambda_{\text{max}} = 520\text{--}540\text{ nm}$ ) and dimeric form ( $\lambda_{\text{max}} = 720\text{--}800\text{ nm}$ ), was observed within the laser pulse. The radical cations decayed by first-order kinetics, and under nitrogen, the formation of ArSCH<sup>•</sup>Ph ( $\lambda_{\text{max}} = 350\text{--}360\text{ nm}$ ) was clearly observed. This indicates that the decay of the radical cation is due to a fragmentation process involving the heterolytic C–C bond cleavage, a conclusion fully confirmed by steady-state photolysis experiments (formation of benzaldehyde and the dimer of the  $\alpha$ -aryl-sulfanyl carbon radical). Whereas the fragmentation rate decreases as the C–C bond dissociation energy (BDE) increases, no rate change was observed by the replacement of OH by OD in the sulfide radical cation ( $k_{\text{OH}}/k_{\text{OD}} = 1$ ). This suggests a transition state structure with partial C–C bond cleavage where the main effect of the OH group is the stabilization of the transition state by hydrogen bonding with the solvent. The fragmentation rate of 2-hydroxy sulfanyl radical cations turned out to be significantly slower than that of nitrogen analogues of comparable reduction potential, probably due to a more efficient overlap between the SOMO in the heteroatom and the C–C bond  $\sigma$ -orbital in the second case. The fragmentation rates of **1**<sup>•+</sup>–**3**<sup>•+</sup> were found to increase by addition of a pyridine, and plots of  $k_{\text{base}}$  against base strength were linear, allowing calculation of the  $\beta$  Brønsted values, which were found to increase as the reduction potential of the radical cation decreases,  $\beta = 0.21$  (**3**<sup>•+</sup>), 0.34 (**1**<sup>•+</sup>), and 0.48 (**2**<sup>•+</sup>). The reactions of **1**<sup>•+</sup> exhibit a deuterium kinetic isotope effect with values that increase as the base strength increases:  $k_{\text{OH}}/k_{\text{OD}} = 1.3$  (pyridine), 1.9 (4-ethylpyridine), and 2.3 (4-methoxypyridine). This finding and the observation that with the above three bases the rate decreases in the order **3**<sup>•+</sup> > **1**<sup>•+</sup> > **2**<sup>•+</sup>, i.e., as the C–C BDE increases, suggest that C–C and O–H bond cleavages are concerted but not synchronous, with the role of OH bond breaking increasing as the base becomes stronger (variable transition state). It is probable that, with the much stronger base, 4-(dimethylamino)pyridine, a change to a stepwise mechanism may occur where the slow step is the formation of a radical zwitterion that then rapidly fragmentates to products.

## Introduction

One of the most important reactions of organic radical cations is the cleavage of a  $\beta$  bond ( $\beta$  with respect to the atom or aromatic ring bearing the positive charge) to produce a cationic species and a free radical (eq 1).



This process has been intensively investigated for some time for its many theoretical aspects and its potential

for a variety of practical applications. From the latter point of view, the fragmentation reactions of radical cations can find use in the initiation of radical polymerizations,<sup>1</sup> the enhancing of silver halide photography efficiency,<sup>2</sup> and organic synthesis.<sup>3</sup> Moreover, these reactions can also be exploited as mechanistic probes to detect

(1) Wrzyszczyński, A.; Filipiak, P.; Hug, G. L.; Marciniak, B.; Pączkowski, J. *Macromolecules* **2000**, *33*, 1577–1582.

(2) (a) Gould, I. R.; Godleski, S. A.; Zielinski P. A.; Farid S. *Can. J. Chem.* **2003**, *81*, 777–788. (b) Gould, I. R.; Lenhard, J. R.; Muentner, A. A.; Godleski, S. A.; Farid, S. *Pure Appl. Chem.* **2001**, *73*, 455–458. (c) Gould, I. R.; Lenhard, J. R.; Muentner, A. A.; Godleski, S. A.; Farid, S. *J. Am. Chem. Soc.* **2000**, *122*, 11934–11943.

(3) Albini, A.; Fagnoni, M.; Mella, M. *Pure Appl. Chem.* **2000**, *72*, 1321–1326.

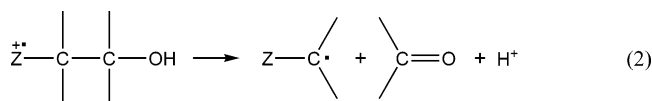
\* Corresponding authors. (E. Baciocchi) Tel: +39-06-49913711. Fax: +39-06-490421. (T. Del Giacco) Tel. +39-075-5855559.

<sup>†</sup> Università “La Sapienza”.

<sup>‡</sup> Università di Perugia.

electron-transfer processes in chemical and biochemical oxidations.<sup>4,5</sup>

A class of radical cation fragmentations that has attracted much attention is that involving the cleavage of a C–C bond assisted by a OH group  $\beta$  with respect to the positively charged moiety (eq 2).



One of the first and more thoughtfully investigated examples of this process concerns the fragmentation reactions of 2-amino alcohol radical cations (i.e., eq 2, Z = R<sub>2</sub>N or ArNH), which was first investigated by Whitten and his associates and then by the Schanze and Mariano groups.<sup>6–9</sup> It was found that the reaction rate is accelerated by bases, with a quite large Brønsted  $\beta$  value (0.62) measured against a series of pyridine bases.<sup>9</sup> The proposed mechanism was that the fragmentation of the radical cation is assisted by an attack of the base at the OH group concerted with the C–C bond cleavage. The possibility of a stepwise mechanism was also suggested where OH deprotonation might precede C–C bond cleavage.

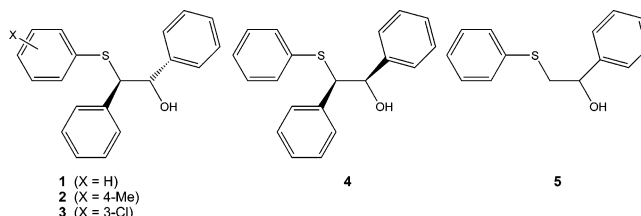
In collaboration with Steen Steenken in Muelheim, our group recently carried out a pulse radiolysis study of the fragmentation reactions of 2-arylethanol radical cations (eq 2, Z = Ar) in water.<sup>10</sup> In basic media, a concerted mechanism similar to that suggested for the amino alcohol radical cations was considered possible, but, since the reaction rate was close to the diffusion-controlled limit, the data were also consistent with the initial formation of an intermediate radical zwitterion.

In the literature, there are a number of reports indicating that the fragmentation described in eq 2 can also be observed in 2-arylsulfanyl alcohol radical cations (eq 2, Z = ArS).<sup>11–14</sup> However, no detailed kinetic study has so far been carried out for these systems and no quantitative information upon their reactivity is presently available.

In view of our continuous interest in the chemistry of radical cations and in the structural factors that determine reactivity and reaction pathways, it was felt that a quantitative investigation of the C–C bond cleavage in 2-arylsulfanyl alcohol radical cations could be warranted.

Apart from furnishing interesting information per se, it should also allow the comparison between nitrogen and sulfur radical cations, thus providing further insight into the energetics and dynamics of a process that is far from being fully understood. Moreover, 2-arylsulfanyl alcohols might be used as clocks to quantitatively assess the role of electron-transfer steps in chemical and biochemical oxidations of sulfides.

In this paper, we report the results of a laser flash and steady-state photolysis study of the *erythro*-1,2-diphenyl-2-arylsulfanylethanol **1–3** in MeCN.



The radical cations were generated by sensitized photolysis in MeCN with *N*-methylquinolinium tetrafluoroborate (NMQ<sup>+</sup>) as the sensitizer. NMQ<sup>+</sup> is a very efficient sensitizer, whose excited state is characterized by a very high reduction potential (2.7 V vs SCE).<sup>15</sup> Moreover, by reacting with the substrate, it forms a radical cation/radical couple whose separation is facilitated by the lack of any electrostatic barrier. To increase the yields in separated radical ions, the laser photolysis experiments were cosensitized by toluene.<sup>16</sup> Some experiments have also been carried out with *threo*-1,2-diphenyl-2-phenylsulfanylethanol (**4**) and with 1-phenyl-2-phenylsulfanylethanol (**5**).

## Results

**Steady-State Photolysis.** Steady-state photolysis sensitized by NMQ<sup>+</sup> was carried out in N<sub>2</sub>-saturated MeCN as described in Experimental Section. No reaction was observed in the absence of sensitizer. Short reaction times (10 min) and an excess of substrate on the sensitizer were used in order to minimize any possible overoxidation. In all cases, the reaction products (comparison with authentic specimens) were determined and quantified by GC, GC-MS, and <sup>1</sup>H NMR.

Irradiation of **1** (1 × 10<sup>−2</sup> M) and NMQ<sup>+</sup> (1 × 10<sup>−3</sup> M) in N<sub>2</sub>-saturated MeCN gave benzaldehyde (40%) and 1,2-bis(phenylsulfanyl)-1,2-diphenylethane (20%) as the exclusive products (the yields were determined with respect to NMQ<sup>+</sup>).<sup>17</sup> The observed outcome can be reasonably rationalized as described in Scheme 1. Formation of the radical cation by photoinduced electron transfer is followed by a heterolytic C–C bond cleavage leading to benzaldehyde and an  $\alpha$ -phenylsulfanyl radical. Dimerization of the latter produces a mixture of *meso*- and *d,l*-1,2-bis(phenylsulfanyl)-1,2-diphenylethane. Similar results were obtained in the steady-state photolysis of **2**

(4) Baciacchi, E.; Lanzalunga, O.; Malandrucchio, S.; Ioele, M.; Steenken, S. *J. Am. Chem. Soc.* **1996**, *118*, 8973–8974.

(5) Baciacchi, E. In *Free Radicals in Biology and Environment*; Minisci, F., Ed.; Kluwer Academic Publishers: Dordrecht, 1997; Nato Asi Series.

(6) Gaillard, E. R.; Whitten, D. G. *Acc. Chem. Res.* **1996**, *29*, 292–297.

(7) Zhuoyi, S.; Mariano, P. S.; Falvey, D. E.; Yoon, U. C.; Oh, S. W. *J. Am. Chem. Soc.* **1998**, *120*, 10676–10686.

(8) Burton, R. D.; Bartberger, M. D.; Zhang, Y.; Eyler, J. R.; Schanze, K. S. *J. Am. Chem. Soc.* **1996**, *118*, 5655–5664 and references therein.

(9) Lucia, L. A.; Burton, R. D.; Schanze, K. S. *J. Phys. Chem.* **1993**, *97*, 9078–9080.

(10) Baciacchi, E.; Bietti, M.; Manduchi, L.; Steenken, S. *J. Am. Chem. Soc.* **1999**, *121*, 6624–6629.

(11) Gravel, D.; Farmer, L.; Ayotte, C. *Tetrahedron Lett.* **1990**, *31*, 63–66.

(12) Vath, P.; Falvey, D. E.; Barnhurst, L. A.; Kutateladze, A. G. *J. Org. Chem.* **2001**, *66*, 2887–2890.

(13) Li, Z.; Kutateladze, A. G. *J. Org. Chem.* **2003**, *68*, 8236–8239.

(14) Ci, X.; Whitten, D. G. In *Photoinduced Electron Transfer*; Fox, M. A.; Chanon, M., Eds.; Elsevier: Amsterdam, 1988; Part C, p 567

(15) Yoon, U. C.; Quillen, S. L.; Mariano, P. S.; Swanson, R.; Stavinoha, J. L.; Bay, E. *J. Am. Chem. Soc.* **1983**, *105*, 1204–1218.

(16) Gould, I. R.; Ege, D.; Mosh, J. E.; Farid, S. *J. Am. Chem. Soc.* **1990**, *112*, 4290–4301.

(17) Same products were observed also when the photolysis was carried out in the presence of O<sub>2</sub>.

## SCHEME 1

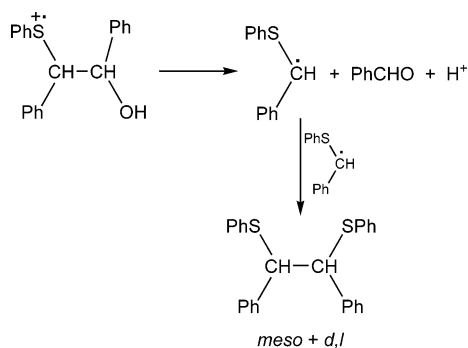


**TABLE 1. Quenching Rate Constants of  $\text{NMQ}^+$  Fluorescence ( $k_q$ ) and Photoreaction Quantum Yields ( $\Phi$ ) of **1**, **2**, and **3** in MeCN**

compound	substituent	$k_q$ ( $10^{10} \text{ M}^{-1} \text{ s}^{-1}$ )	$\Phi$
<b>2</b>	$-\text{CH}_3$	2.7	0.26
<b>1</b>	$-\text{H}$	2.0	0.49
<b>3</b>	$-\text{Cl}$	1.8	0.62

and **3** and also when the reaction was carried out in the presence of pyridine.

No products were observed, however, when **5** was irradiated under identical conditions. In the presence of pyridine, too, **5** was much less reactive than **1**. Accordingly, in the simultaneous irradiation (10 min) of two separate solutions ( $1 \times 10^{-2} \text{ M}$ ) of **1** and **5** with  $\text{NMQ}^+$  ( $5 \times 10^{-3} \text{ M}$ ) and pyridine ( $1 \times 10^{-2} \text{ M}$ ) in  $\text{N}_2$ -saturated MeCN, benzaldehyde was obtained from **1** in 16% yield (16% conversion) with respect to the substrate, while from **5**, the yield in benzaldehyde was only 0.5%.

Quantum yields ( $\Phi$ ) for the photolysis of **1–3**, under the conditions listed above, were also determined on the basis of the formation of benzaldehyde. The results, reported in Table 1, indicate that the reaction is quite efficient, with values of  $\Phi$  between 0.26 (**2**) and 0.62 (**3**).

**Fluorescence Quenching.** Fluorescence-quenching experiments were carried out in  $\text{N}_2$ -saturated MeCN to determine the efficiency by which substrates **1–3** quench the lowest excited singlet state of  $\text{NMQ}^+$ . The fluorescence intensity of  $\text{NMQ}^+$  was recorded by steady-state experiments in the absence ( $I_F^\circ$ ) and in the presence ( $I_F$ ) of increasing concentrations of the substrates ( $S$ ). Table 1 lists the second-order rate constants for  $\text{NMQ}^+$  fluorescence quenching ( $k_q$ ) calculated from the slopes of the linear Stern–Volmer plots ( $I_F^\circ/I_F$  vs  $[S]$ ) divided by the lifetime of  $^1\text{NMQ}^{+*}$  (20 ns).<sup>18</sup> The Stern–Volmer plots show that each substrate efficiently quenches the emission of  $\text{NMQ}^+$ , presumably via a diffusion-controlled electron-transfer process. This behavior is in line with the laser flash photolysis experiments where the radical cations of **1–3** were produced within the laser pulse (see below).

**Laser Flash Photolysis Studies.** The laser photolysis experiments were carried out in the presence of 1 M toluene as a cosensitizer. Upon laser excitation ( $\lambda_{\text{exc}} = 308$  and/or 355 nm) of MeCN solutions of  $\text{NMQ}^+$ /toluene/**1–4**, time-resolved absorption spectra and decay kinetics were recorded under  $\text{N}_2$ - and  $\text{O}_2$ -saturated conditions.

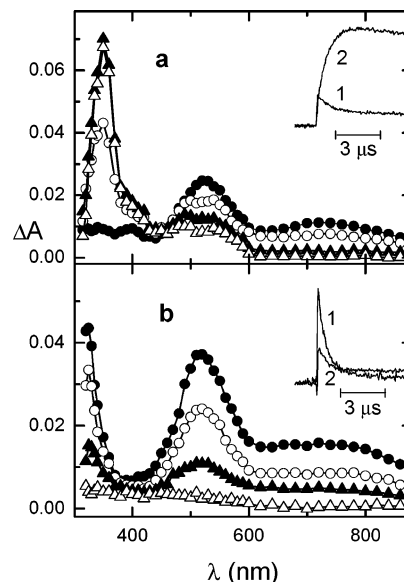


**FIGURE 1.** Time-resolved absorption spectra of the  $\text{NMQ}^+$  ( $8 \times 10^{-5} \text{ M}$ )/toluene (1 M)/**1** ( $5 \times 10^{-3} \text{ M}$ ) system in MeCN: (a)  $\text{N}_2$ -saturated, recorded 0.032 (●), 0.46 (○), 1.8 (▲), and 6.4 (△)  $\mu\text{s}$  after the laser pulse and (b)  $\text{O}_2$ -saturated, recorded 0.08 (●), 0.4 (○), 0.9 (▲), and 6.4 (△)  $\mu\text{s}$  after the laser pulse. Insets: decay kinetics recorded at 520 nm (1) and 350 nm (2).  $\lambda_{\text{exc}} = 308 \text{ nm}$ .

Since the results were very similar for all sulfides examined, only those concerning the unsubstituted sulfide **1** will be illustrated in detail.

By laser photolysis of **1** in  $\text{N}_2$ -saturated solutions, three absorption bands were detected just after the laser pulse in the 400 (a shoulder), 520, and 700 nm regions (Figure 1). They were assigned to  $\text{NMQ}^+$  ( $\lambda_{\text{max}} = 400$  and 550 nm)<sup>19</sup> and the monomer ( $\lambda_{\text{max}} = 520 \text{ nm}$ ) and the dimer sulfide radical cations ( $\lambda_{\text{max}} \approx 720 \text{ nm}$ ).<sup>20</sup> The time-evolution of the absorption spectra shows that the signal decay recorded at ca. 400 and 520 nm is coupled with the growth of an additional maximum at 350 nm region assigned to the absorption of the radical  $\text{PhSCH}^+\text{Ph}$ <sup>21</sup> (Figure 1a, inset); accordingly, in  $\text{O}_2$ -saturated solutions, the time-resolved absorption spectra are modified by the fast decay of  $\text{PhSCH}^+\text{Ph}$  and  $\text{NMQ}^+$ , which are efficiently quenched by molecular oxygen; thus, the shoulder at ca. 400 nm disappears and the only recorded transient concerns the radical cation in its monomeric ( $\lambda_{\text{max}} = 520 \text{ nm}$ ) and dimeric ( $\lambda_{\text{max}} \approx 720 \text{ nm}$ , Figure 1b) forms. Clearly, the observation of  $\text{PhSCH}^+\text{Ph}$  fully confirms the results of the steady-state experiments, indicating that the decay of the radical cation is due to a fragmentation process involving the heterolytic C–C bond cleavage (Scheme 1).

The decay rate of radical cations **1**<sup>+</sup>–**4**<sup>+</sup> was determined by following, in the presence of nitrogen, the absorption rise at 350 nm (due to the carbon radical) and, in the presence of oxygen, the absorption decay at 520

(19) Bockman, T. M.; Kochi, J. K. *J. Am. Chem. Soc.* **1989**, *111*, 4669–4683.

(20) Yokoi, H.; Hatta, A.; Ishiguro, K.; Sawaki, Y. *J. Am. Chem. Soc.* **1998**, *120*, 12728–12733.

(21) Actual absorption spectrum of  $\text{PhSCH}^+\text{Ph}$  was obtained by photolysis of  $\text{PhSCH}_2\text{Ph}$  (0.01 M) and di-*tert*-butyl peroxide (0.5 M) in MeCN ( $\lambda_{\text{exc}} = 308 \text{ nm}$ ).

(18) Fukuzumi, S.; Fujita, M.; Noura, S.; Ohkubo, K.; Suenobu, T.; Araki, Y.; Ito, O. *J. Phys. Chem. A* **2001**, *105*, 1857–1868.

**TABLE 2.** Decay Rate Constants and Activation Energies for Fragmentation of the Sulfide Radical Cations in MeCN

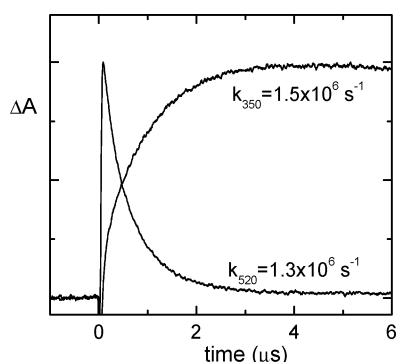
radical cation	substituent	$k_{fr}$ ( $10^6$ s $^{-1}$ )	$\Delta H^\ddagger$ (kcal mol $^{-1}$ K $^{-1}$ )	$\Delta S^\ddagger$ (cal mol $^{-1}$ K $^{-1}$ )	$E^\circ_{red}$ (V) <sup>a</sup>
<b>2</b> <sup>+</sup>	–CH <sub>3</sub>	0.26	5.9 ± 0.8	–15 ± 4	1.43
<b>1</b> <sup>+</sup>	–H	1.3	6.2 ± 0.7	–9 ± 3	1.55
<b>3</b> <sup>+</sup>	–Cl	11	5.7 ± 0.8	–7 ± 3	1.67
<b>4</b> <sup>+</sup>		0.71			

<sup>a</sup> Versus SCE in MeCN, taken equal to those of the corresponding ArSCH<sub>2</sub>Ph<sup>+</sup>.<sup>22</sup>

**TABLE 3.** Decay Rate Constants ( $k_{base}$ ) and Brønsted Parameters ( $\beta$ ) for the Base-Catalyzed Fragmentation of the Sulfide Radical Cations in MeCN

radical cation	substituent	$k_{base}$ ( $10^8$ M $^{-1}$ s $^{-1}$ )				$\beta^b$
		pyridine (pK <sub>a</sub> = 12.33) <sup>a</sup>	4-Et-pyridine (pK <sub>a</sub> = 13.35) <sup>a</sup>	4-MeO-pyridine (pK <sub>a</sub> = 14.04) <sup>a</sup>	4-Me <sub>2</sub> N-pyridine (pK <sub>a</sub> = 17.74) <sup>a</sup>	
<b>2</b> <sup>+</sup>	–CH <sub>3</sub>	0.13	0.25	0.43	44	0.48
<b>1</b> <sup>+</sup>	–H	1.1	1.6	3.0	64	0.34
<b>3</b> <sup>+</sup>	–Cl	3.6	5.7	6.6	46	0.21
<b>4</b> <sup>+</sup>		0.55				

<sup>a</sup> pK<sub>a</sub> in MeCN.<sup>23</sup> <sup>b</sup> Slope of the log  $k_{base}$  vs pK<sub>a</sub> plot.

**FIGURE 2.** Normalized decay kinetics of the NMQ<sup>+</sup> ( $8 \times 10^{-5}$  M)/toluene (1 M)/**1** ( $5 \times 10^{-3}$  M) system in MeCN recorded in O<sub>2</sub>- and N<sub>2</sub>-saturated solutions at 520 and 350 nm, respectively.

nm (due to the radical cation). In both cases, the decay kinetics followed first order laws and provided almost identical values of the decay rate constants (see Figure 2). In some cases, particularly for **1**, the decay rate of the radical cation was also measured by following the absorption changes of the dimer radical cation. The decay rate constants ( $k_{fr}$ ), for all the radical cations, measured at 25 °C are reported in Table 2. The activation parameters ( $\Delta H^\ddagger$  and  $\Delta S^\ddagger$ ) for the fragmentation process of **1**<sup>+</sup>–**3**<sup>+</sup> (Table 2) were determined over the temperature range from 258 to 358 K by Eyring plots analysis (see Supporting Information for the Eyring plots and further spectral data of the investigated radical cations). It appears that bond fragmentation in the radical cations **1**<sup>+</sup>–**3**<sup>+</sup> is characterized by both low activation enthalpies and negative activation entropies. Laser photolysis of **5** in the presence of NMQ<sup>+</sup> and 1 M toluene also produced **5**<sup>+</sup> (monomer at 530 nm and dimer at 750 nm). However, in this case, the decay of **5**<sup>+</sup>, significantly slower than that of **1**<sup>+</sup>, exhibited mixed first-order/second-order kinetics, indicating that the decay is to some extent influenced by radical–radical reactions. Thus, no reliable rate constant for the fragmentation rate of **5**<sup>+</sup> could be determined.

Some experiments were carried out in MeCN with 1% H<sub>2</sub>O and in MeCN with 1% D<sub>2</sub>O using **1** as the substrate. Identical values of  $k_{fr}$  ( $1.6 \times 10^6$  s $^{-1}$ ) were found under

the two conditions, thus indicating the absence of any significant kinetic isotope effect when OH is replaced by OD.

Addition of pyridine or substituted pyridines accelerates the decay rate of radical cations; according to eq 3, linear plots were obtained by reporting the first-order rate constants ( $k_{obs}$ ) versus base concentration ([base]), which provided us with the second-order rate constants ( $k_{base}$ ) for the base-promoted reactions (Table 3).

$$k_{obs} = k_{fr} + k_{base}[base] \quad (3)$$

The  $k_{base}$  values increase as the base strength increases, in good accord with the Brønsted equation (Figure S2, Supporting Information). The Brønsted  $\beta$  parameters, which was observed to be significantly different for **1**<sup>+</sup>, **2**<sup>+</sup>, and **3**<sup>+</sup>, are also reported in Table 3.

The effect of replacing OH by OD in the sulfide was also studied in the presence of pyridine. In this case, the fragmentation of **1**<sup>+</sup> is faster in MeCN–1% H<sub>2</sub>O than in MeCN–1% D<sub>2</sub>O ( $9.7 \times 10^7$  M $^{-1}$  s $^{-1}$  vs  $5.0 \times 10^7$  M $^{-1}$  s $^{-1}$ ). From these values, a deuterium kinetic isotope effect ( $k_{OH}/k_{OD}$ ) of 1.9 was calculated.

## Discussion

**Fragmentations in the Absence of Bases.** NMQ<sup>+</sup> has been confirmed to be an excellent sensitizer for the photoinduced generation of aromatic sulfide radical cations. Accordingly, the rates of fluorescence quenching are diffusion-controlled (Table 1) and the quantum yields for the photoreaction of **1**–**3** are also relatively large (0.26–0.62, Table 1). As expected, the quantum yields increase in the order **2** < **1** < **3**, that is, as the fragmentation rate of the radical cation increases (see below), thus better competing with back-electron transfer.

Looking first at the effect of ring substituents on the fragmentation rate constants, we note that  $k_{fr}$  increases in the order **2**<sup>+</sup> < **1**<sup>+</sup> < **3**<sup>+</sup>, that is as the  $E^\circ_{red}$  of the radical cations increases (Table 2). This observation is in line with expectations because increasing the  $E^\circ_{red}$  of the radical cation leads to a corresponding decrease in

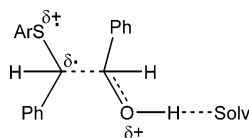


**FIGURE 3.** Transition state structure for the fragmentation of a 2-arylsulfanyl alcohol radical cation in the absence of base.

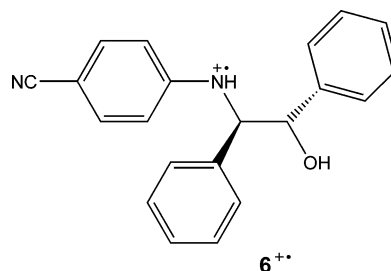
the heterolytic bond dissociation energy (BDE)<sup>24</sup> of the C–C bond (Scheme 1). Accordingly, by DFT calculations BDEs (kcal mol<sup>−1</sup>) were found to be: 36.9 for **2**<sup>+</sup>, 33.2 for **1**<sup>+</sup>, and 29.1 for **3**<sup>+</sup>.

The activation parameters displayed in Table 2 confirm previous observations that the fragmentation reactions of radical cations are characterized by a negative entropy of activation, which has been attributed to the partial formation of a double bond in the transition state<sup>6</sup> and/or to the stereoelectronic requirements of the process (vide infra).<sup>8</sup> In our case, it would seem that differences in reactivity are mostly related to the entropic factor, but this may be due to the considerable experimental errors, inherent to this type of determination.

The observation that the fragmentation rates decrease as the C–C BDE increases suggests that some degree of C–C bond breaking must occur in the transition state of the fragmentation process. This conclusion is fully supported also by the finding that the fragmentation of **5**<sup>+</sup> must be significantly slower than that of **1**<sup>+</sup> since no products were obtained in the steady-state photolysis of **5**. In **5**<sup>+</sup>, the absence of the 2-phenyl group significantly increases the C–C BDE by 9.3 kcal mol<sup>−1</sup> with respect to that in **1**<sup>+</sup>.

The same reactivity, however, has been observed when the alcoholic OH group is replaced by OD, which suggests that, in the absence of bases, the rupture of the O–H bond is not associated with the cleavage of the C–C bond. Thus, as previously suggested for the fragmentations of arylalkanol radical cations in water<sup>10</sup> and also in the case of 2-arylsulfanyl alcohol radical cations, the favorable effect of the OH group with respect to C–C bond cleavage<sup>25</sup> might be due to a stabilization of the transition state by hydrogen bonding with the solvent.<sup>26</sup> The transition state structure might be that represented in Figure 3,<sup>28</sup> where there is a partial cleavage of the C–C bond and a partial positive charge on oxygen, thus allowing partial formation of the carbon oxygen double bond.<sup>29</sup>

It is certainly of interest to compare the reactivity of 2-arylsulfanyl alcohol radical cations with that of 2-hydroxy anilinium analogues. To make a meaningful comparison, however, radical cations of comparable stability and studied in the same solvent should be considered. These requirements are substantially fulfilled if we compare the reactivity of **2**<sup>+</sup> ( $E_{\text{red}} = 1.4$  V vs SCE) with that of the 4-cyanoanilinium radical cation **6**<sup>+</sup> ( $E_{\text{red}} = 1.3$  V vs SCE) determined by Schanze in MeCN.<sup>8</sup> The result is that **6**<sup>+</sup> is much more reactive than **2**<sup>+</sup> ( $7.4 \times 10^6$  s<sup>−1</sup> vs  $2.6 \times 10^5$  s<sup>−1</sup>). Since the C–C BDEs are very similar for **2**<sup>+</sup> and **6**<sup>+</sup>, 36.9 and 34.6 kcal mol<sup>−1</sup>, respectively (by DFT calculations), we attribute the higher reactivity of **6**<sup>+</sup> with respect to **2**<sup>+</sup> to a more efficient overlap between the SOMO of the radical cation and the 2p  $\sigma$ -orbital of the scissile C–C bond when the SOMO is on nitrogen (2p orbital) than when it is on sulfur (3p orbital), due to the better matching of the energies in the former case. Such an overlap is essential for the intramolecular electron-transfer process, from the C–C bond to the SOMO on the heteroatom, which has to accompany the C–C bond cleavage.



**Base-Promoted Fragmentations.** As in the case of 2-amino alcohol and 2-phenylethanol radical cations, the fragmentation rate of 2-sulfanyl alcohol radical cations is accelerated by the presence of a base. The second-order rate constants for the decay of **1**<sup>+</sup>–**3**<sup>+</sup> in the presence of pyridine bases ( $k_{\text{base}}$ ) and the Brønsted  $\beta$  values are displayed in Table 3.

Differently than for the fragmentations in the absence of bases, the reaction of **1**<sup>+</sup> promoted by pyridine, 4-ethylpyridine, and 4-methoxypyridine exhibits a deuterium kinetic isotope effect when the alcoholic OH is replaced by OD, with values that increase as the base strength increases:  $k_{\text{OH}}/k_{\text{OD}} = 1.3$  (pyridine), 1.9 (4-ethylpyridine), and 2.3 (4-methoxypyridine).<sup>30</sup> This finding and the observation that, with the above three bases, the rate decreases in the order expected on the basis of C–C BDEs (i.e. **3**<sup>+</sup> > **1**<sup>+</sup> > **2**<sup>+</sup>), suggest a transition state structure where C–C bond cleavage and the intramolecular electron transfer from the scissile bond to the sulfur atom are to some extent coupled with the base-induced OH bond breaking. The more logical hypothesis is that, in this case, the 2-arylsulfanyl alcohol radical cations fragment by the same concerted mechanism (Figure 4, Grob-type fragmentation) proposed by the Whitten and Schanze groups for the corresponding reactions of amino alcohol radical cations.<sup>6,8</sup>

(22) Baciocchi, E.; Intini, D.; Piermattei, A.; Rol, C.; Ruzziconi, R. *Gazz. Chim. Ital.* **1989**, *119*, 649–652.

(23) (a) Kaliurand, I.; Rodima, T.; Leito, I.; Koppel, I.; Schwesinger, R. *J. Org. Chem.* **2000**, *65*, 6202–6208. (b) Savelova, V. A.; Popov, A. F.; Solomoichenko, T. N.; Sadvovskii, Y. S.; Piskunova, Z. P.; Lobanova, O. V. *Russ. J. Org. Chem.* **2000**, *36*, 1465–1473.

(24) This refers to the C–C bond cleavage in the radical cation leading to  $\alpha$ -sulfanyl-substituted radical and the protonated benzaldehyde.

(25) The OH group must certainly have a role, as no fragmentation occurs in its absence.

(26) In the formation of hydrogen bonds, replacement of hydrogen by deuterium does not significantly affect the equilibrium constant between the free and the hydrogen bonded species.<sup>27</sup>

(27) (a) Vinogradov, S. N.; Linnell, R. H. In *Hydrogen Bonding*; Van Nostrand Reinhold Company: New York, 1971; p 124. (b) Joesten, M. D.; Schaad, L. J. In *Hydrogen Bonding*; Marcel Dekker: New York, 1974; Appendix.

(28) Since the experiments to determine the  $k_{\text{OH}}/k_{\text{OD}}$  isotope effect were carried out in MeCN containing 1% H<sub>2</sub>O or 1% D<sub>2</sub>O (see Experimental Section), it might be that under these conditions “Solv” in Figure 3 is H<sub>2</sub>O or D<sub>2</sub>O.

(29) As suggested by a referee, our observations might also be consistent with a very early transition state with respect to OH bond breaking.

(30) Addition of water induced an increase in the fragmentation rate of **1**<sup>+</sup>, so that the rates became too fast to be measured with the necessary precision.

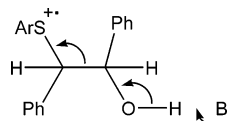


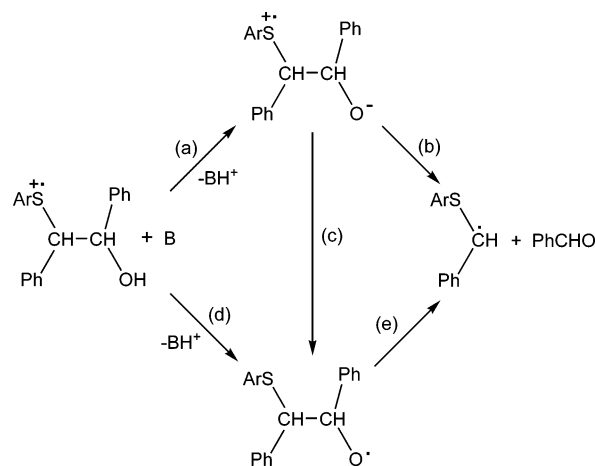
**FIGURE 4.** Transition state structure for the base-promoted fragmentation of a 2-arylsulfanyl alcohol radical cation.

However, the observed increase of  $k_{\text{OH}}/k_{\text{OD}}$  as the base becomes stronger clearly indicates that the structure of the transition state in Figure 4 has to be variable. Namely, as we move to stronger bases, the role of the cleavage of the OH bond in the transition state becomes progressively more important than the cleavage of the C–C bond. In other words, the bond cleavage in the transition state is concerted but not synchronous. Following the language used in  $\beta$ -elimination reactions, to which these fragmentation have been correctly assimilated,<sup>8</sup> these transition states might be indicated as E1cb-like.

As suggested for the reactions of anilinium radical cations,<sup>8,9,31</sup> the concerted mechanism reported in Figure 4 should be favored by an anti relationship between the charged sulfur and the hydroxy oxygen and the C<sub>1</sub> and C<sub>2</sub> phenyl groups (stereoelectronic effect). Indeed, we found that with pyridine, the *erythro* form **1**<sup>+</sup> is about 2 times more reactive than the *threo* form **4**<sup>+</sup> (Table 3), in agreement with the fact that the above-mentioned anti relationship can be better obtained in the *erythro* than in the *threo* diastereomer (vide infra). However, practically the same difference in the reactivity between the two diastereomers has also been observed in the absence of bases (Table 2), where the mechanism should not involve O–H bond breaking in the transition state. Furthermore, DFT calculations (Supporting Information) show that in order to reach the conformation with anti OH and phenylsulfanyl groups, starting from the conformation with the absolute minimum of energy (where the OH and the phenylsulfanyl groups are gauche), **4**<sup>+</sup> has to spend ca. 3 kcal mol<sup>−1</sup> more than **1**<sup>+</sup>. Thus, were stereoelectronic effects important, the difference in the fragmentation rate of the two diastereomers would be much higher than that actually observed. In conclusion, stereoelectronic effects seem to play a very minor role in the fragmentation of 2-phenylsulfanyl alcohol radical cations, probably due to a process that, as said before, is shifted to the E1cb side of the mechanistic spectrum.

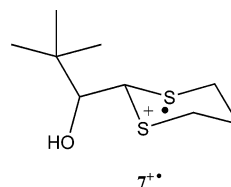
Given this situation, it is conceivable that by further increasing the strength of the base, a limit can be reached where we pass from a concerted to a stepwise mechanism where the slow step is the formation of a radical zwitterion (and accordingly the rate is almost diffusion controlled) that then undergoes fast C–C bond cleavage to the reaction products (E1cb mechanism, Scheme 2, paths a and b). This probably occurs with the much stronger base, 4-(dimethylamino)pyridine (DMAP), since with this base, **1**<sup>+</sup>, **2**<sup>+</sup>, and **3**<sup>+</sup> react at practically the same rate,<sup>32</sup> as predicted by the stepwise mechanism (Scheme 2, paths a and b). An alkoxyl radical that undergoes a fast  $\beta$ -fragmentation might also be involved as a reaction

## SCHEME 2



intermediate, but it should be formed in a fast step following the formation of the radical zwitterion (Scheme 2, paths a, c, and e). A slow formation of the alkoxyl radical (Scheme 2, paths d and e) should exhibit a rate dependence on the stability of the radical cation, which is not observed.<sup>33</sup>

In this respect, it is interesting to note that convincing evidence for the formation of an alkoxyl intermediate in a fragmentation of 2-hydroxy sulfanyl radical cation has been presented recently by Li and Kutateladze for the case of 2-( $\alpha$ -hydroxyneopentyl)-1,3-dithianyl radical cation (**7**<sup>+</sup>).<sup>13</sup> In this system, the sulfur atoms are part of a six-member cycle and it is possible that there is a kinetic barrier for the Grob fragmentation because of orbital misalignment between the SOMO on sulfur and the scissile C–C bond. This results in a stepwise fragmentation mechanism with the slow formation of the alkoxyl radical.



## Summary and Conclusions

By laser flash and steady-state photolysis studies, the formation of 2-arylsulfanyl alcohol radical cations **1**<sup>+</sup>–**4**<sup>+</sup> and their C–C bond fragmentation, a heterolytic-type process affording an  $\alpha$ -phenylsulfanyl-substituted carbon radical and benzaldehyde, has been shown. The fragmentation reactions exhibit first-order kinetics with rates that increase as the C–C bond dissociation energy (BDE) in the radical cation decreases. Since the fragmentation rate remains the same when the alcoholic OH is replaced by OD ( $k_{\text{OH}}/k_{\text{OD}} = 1$ ), a transition state structure is suggested with partial C–C bond cleavage and an intact

(31) Ci, X.; Kellett, M. A.; Whitten, D. G. *J. Am. Chem. Soc.* **1991**, *113*, 3893–3894.

(32) With bases stronger than DMAP, the fragmentation rate was too fast to be measured with our laser flash photolysis apparatus.

(33) One might also suggest that the mechanism is stepwise (Scheme 2, paths a, c, and e) with all bases and that the slow step is the formation of the zwitterion (path a) with the stronger base, 4-(dimethylamino)pyridine, whereas it is the formation of the alkoxyl radical (step c) with the other bases. However, in the latter case the formation of the zwitterion should be reversible and no clean first-order kinetics should have been observed due to a retarding effect of the protonated base.

O–H bond. Such a transition state can be stabilized by formation of a hydrogen bond between the partially positive OH group and the solvent. It was found that the fragmentation rate of a 2-sulfanyl alcohol radical cation is significantly lower than that of a structurally similar 2-hydroxy anilinium radical cation, which has similar C–C BDE values. The difference is attributed to a less efficient overlap between the SOMO in the heteroatom and the s-orbital of the scissile C–C bond in the sulfide radical cation than in the nitrogen counterpart.

The fragmentation rates of  $1^{+\bullet}$ – $4^{+\bullet}$  increase in the presence of pyridine, and the second-order rate constants for the base-induced process correlate with the base strength, providing  $\beta$  Brønsted values that increase as the  $E^{\circ}_{\text{red}}$  of the radical cation decreases. In the base-assisted process, a deuterium kinetic isotope effect,  $k_{\text{OH}}/k_{\text{OD}}$ , is observed that increases with the strength of the base: pyridine (1.3), 4-ethylpyridine (1.9), and 4-methoxy-pyridine (2.3). This finding and the observation that with the above three bases the rate decreases as the C–C BDE increases suggest that C–C and O–H bond cleavages are concerted but not synchronous, with the role of OH bond breaking increasing as the base becomes stronger (variable transition state). Accordingly, this reaction appears to exhibit very small stereoelectronic requirements (anti relationship between the sulfanyl and OH groups), as  $1^{+\bullet}$  (*erythro*) is only 2 times more reactive than the *threo* diastereomer  $4^{+\bullet}$ . With the much stronger base 4-(dimethylamino)pyridine, a stepwise mechanism, involving the formation of a zwitterion that then undergoes fragmentation, seems more probable. Accordingly, with this base the fragmentation rate turns out to be independent of the C–C BDE.

## Experimental Section

**Materials.** 2-(Phenylsulfanyl)ethanol was purchased and used as received. 1,2-Bis(phenylsulfanyl)-1,2-diphenylethane (a 1:1 *meso/d,l* mixture) was prepared according to literature procedure.<sup>34,35</sup> *N*-Methylquinolinium tetrafluoroborate was prepared according to a literature procedure.<sup>36</sup> Acetonitrile and toluene were used as received.

***erythro*-1,2-Diphenyl-2-arylsulfanylethanols (1–3).** *trans*-Stilbene oxide (20 mmol), potassium carbonate (21 mmol), and the corresponding substituted thiophenol in ethanol (95%, 30 mL) were refluxed for 2.5 h, after which the mixture was cooled and poured in water (20 mL) and extracted three times with diethyl ether (3  $\times$  20 mL). The collected organic layers were then washed with diluted NaOH (100 mL) and with water, dried over anhydrous  $\text{Na}_2\text{SO}_4$ , evaporated, and purified by silica gel chromatography (petroleum ether–ethyl acetate, gradient 1:0 to 4:1).

***threo*-1,2-Diphenyl-2-phenylsulfanylethanol (4).** The synthetic procedure is identical to that reported above for the corresponding *erythro* isomer with the exception that *cis*-stilbene was used. After purification, a colorless waxy solid was obtained (68% yield).

**1-Phenyl-2-phenylsulfanylethanol (5).** Styrene oxide (42 mmol) was slowly added to a stirred solution of thiophenol (38 mmol) and potassium carbonate (58 mmol). The mixture was refluxed for 2.5 h. The workup and purification procedures were identical to those reported above for the *erythro*-1,2-

diphenyl-2-arylsulfanylethanols. 1-Phenyl-2-phenylsulfanylethanol and 2-phenyl-2-phenylsulfanylethanol were both present in the crude reaction mixture. 1-Phenyl-2-phenylsulfanylethanol (48% yield) was obtained as a colorless oil.

**Steady-State Photooxidation: General Procedure.** Photooxidation reactions were carried out in a Rayonet reactor equipped with 16 lamps (3500 Å; 24 W each). A solution containing the 2-arylsulfanyl alcohol ( $1 \times 10^{-2}$  M) and  $\text{NMQ}^+$  ( $1 \times 10^{-3}$  M) in  $\text{N}_2$ -saturated MeCN was irradiated in a rubber cap-sealed, jacketed tube for 10 min, thermostated at 25 °C by a Peltier apparatus. An internal standard (4-methylbenzophenone) was added, and product analysis (comparison with authentic specimens) was carried out by GC, GC-MS, and  $^1\text{H}$  NMR. In the case of photooxidations in the presence of pyridine ( $1 \times 10^{-2}$  M), the procedures were the same with the exception that more  $\text{NMQ}^+$  ( $5 \times 10^{-3}$  M) was used.

**Fluorescence Quenching.** Measurements were carried out on spectrofluorometer. Relative emission intensities at 390 nm ( $\text{NMQ}^+$  emission maximum) were measured irradiating at 315 nm ( $\text{NMQ}^+$  absorption maximum) and 25 °C a solution containing  $\text{NMQ}^+$  ( $5 \times 10^{-5}$  M) with the substrate at different concentrations (from 0 to  $5 \times 10^{-4}$  M) in MeCN degassed by argon.

**Laser Flash Photolysis.** Excitation wavelengths of 308 nm (from a XeCl excimer laser, Lambda Physik, pulse width ca. 15 ns and energy <3 mJ per pulse) and 355 nm (from a Nd:YAG laser, Continuum, third harmonic, pulse width ca. 7 ns and energy <3 mJ per pulse) were used in nanosecond flash photolysis experiments.<sup>37,38</sup>

The transient spectra were obtained by a point-to-point technique, monitoring the change of absorbance ( $\Delta A$ ) after the laser flash at intervals of 5–10 nm over the spectral range 300–900 nm, averaging at least 10 decays at each wavelength. The lifetime values (the time at which the initial signal is reduced to  $1/e$ , experimental error of  $\pm 10\%$ ) are reported for transients showing first-order decay kinetics. All solutions were flowed through a quartz photolysis cell while nitrogen or oxygen was bubbling through them. All measurements were carried out at  $22 \pm 2$  °C unless otherwise indicated.

**Quantum Yields.** A 3 mL solution of  $\text{NMQ}^+$  ( $8.8 \times 10^{-4}$  M) and **1–3** ( $1.0 \times 10^{-2}$  M) in  $\text{N}_2$ -saturated MeCN was placed in a quartz cell and irradiated at 313 nm, selected with a Balzer interference filter by a high-pressure Hg lamp. The photoproducts were quantified by GC analysis by use of 4-methyl-benzophenone as an internal standard. The substrate conversion was held below 10% to avoid secondary reactions. The light intensity (ca.  $4 \times 10^{14}$  photons  $\text{s}^{-1}$ ) was measured by potassium ferric oxalate actinometry.

**DFT Calculation of Radical Cation BDE Values.** The C–C heterolytic bond dissociation energies (BDEs) for the radical cations were determined by quantum chemical calculations accomplished by the Gaussian 98 package.<sup>39</sup> All geometries were optimized at the B3LYP/6-31G(d) level.<sup>40,41</sup> Single-

(37) Romani, A.; Elisei, F.; Masetti, F.; Favaro, G. *J. Chem. Soc., Faraday Trans.* **1992**, 88, 2147–2154.

(38) Görner, H.; Elisei, F.; Aloisi, G. G. *J. Chem. Soc., Faraday Trans.* **1992**, 88, 29–34.

(39) Frisch, M. J.; Trucks, G. W.; Schlegel, H. B.; Scuseria, G. E.; Robb, M. A.; Cheeseman, J. R.; Zakrzewski, V. G.; Montgomery, J. A., Jr.; Stratmann, R. E.; Burant, J. C.; Dapprich, S.; Millam, J. M.; Daniels, A. D.; Kudin, K. N.; Strain, M. C.; Farkas, O.; Tomasi, J.; Barone, V.; Cossi, M.; Cammi, R.; Mennucci, B.; Pomelli, C.; Adamo, C.; Clifford, S.; Ochterski, J.; Petersson, G. A.; Ayala, P. Y.; Cui, Q.; Morokuma, K.; Malick, D. K.; Rabuck, A. D.; Raghavachari, K.; Foresman, J. B.; Cioslowski, J.; Ortiz, J. V.; Stefanov, B. B.; Liu, G.; Liashenko, A.; Piskorz, P.; Komaromi, I.; Gomperts, R.; Martin, R. L.; Fox, D. J.; Keith, T.; Al-Laham, M. A.; Peng, C. Y.; Nanayakkara, A.; Gonzalez, C.; Challacombe, M.; Gill, P. M. W.; Johnson, B. G.; Chen, W.; Wong, M. W.; Andres, J. L.; Head-Gordon, M.; Replogle, E. S.; Pople, J. A. *Gaussian 98*, revision A.7; Gaussian, Inc.: Pittsburgh, PA, 1998.

(40) Parr, R. G.; Yang, W. In *Density-Functional Theory of Atoms and Molecules*; Oxford University Press: New York, 1989.

(34) Alnajjar, M. S.; Franz, J. A. *J. Am. Chem. Soc.* **1992**, 114, 1052–1058.

(35) Kauffman, T. *Angew. Chem., Int. Ed. Engl.* **1974**, 13, 291–304.

(36) Donovan, P. F.; Conley, D. A. *J. Chem. Eng. Data* **1966**, 11, 614.

point energies for the optimized structures were computed using the MPW1P86 functional<sup>42</sup> and the same basis set.

**Conformational Analysis.** For all species, optimized geometries were determined at the B3LYP/6-31G(d) level<sup>40,41</sup> by using a variety of different starting geometries in order to minimize the possibility of finding structures that correspond to a local but not a global energy minimum. In the energy-minimized structure of the *erythro* radical cation (**1**<sup>•+</sup>) the phenylsulfanyl and the OH groups are gauche, while the anti conformer is only a local minimum, located 2.2 kcal mol<sup>-1</sup> above the absolute minimum. A qualitatively similar situation has been found even for the threo radical cation (**4**<sup>•+</sup>), but with this diastereomer the energy difference between the gauche and the anti conformations is higher (5.7 kcal mol<sup>-1</sup>).

(41) Hehre, W. J.; Radom, L.; Schleyer, P. v. R.; Pople, J. A. *Ab Initio Molecular Orbital Theory*; J. Wiley & Sons: New York, 1987.

(42) Yao, X.-Q.; Hou, X.-J.; Jiao, H.; Xiang, H.-W.; Li, Y.-W. *J. Phys. Chem. A* **2003**, *107*, 9991.

**Acknowledgment.** MIUR, University “La Sapienza” of Rome, and University of Perugia are thanked for the financial support.

**Supporting Information Available:** Absorption maxima and transients produced by LFP of NMQ<sup>+</sup>/toluene/sulfide in N<sub>2</sub>-saturated MeCN; temperature effect on the decay rate constant ( $k_{\text{fr}}$ ) of **2**<sup>•+</sup>, **1**<sup>•+</sup>, and **3**<sup>•+</sup> in MeCN; Brønsted plot (log  $k_{\text{base}}$  vs p*K*<sub>a</sub>) for fragmentation of **2**<sup>•+</sup>, **1**<sup>•+</sup>, and **3**<sup>•+</sup> in MeCN; analytical and spectroscopic data for compounds **1–5**; and optimized geometries (Cartesian coordinates) and calculated energies for **1**<sup>•+</sup>–**5**<sup>•+</sup> and their fragmentation products. This material is available free of charge via the Internet at <http://pubs.acs.org>.

JO0486544